Clays and Clay Minerals, Vol. 46, No. 4, 466–477, 1998.

COMBINATION BANDS IN THE INFRARED SPECTROSCOPY OF KAOLINS—A DRIFT SPECTROSCOPIC STUDY

RAY L. FROST AND URSULA JOHANSSON†

Centre for Instrumental and Developmental Chemistry, Queensland University of Technology, 2 George Street, GPO Box 2434, Brisbane Queensland 4001, Australia

Abstract—Kaolinites with varying degrees of defect structures have been studied by both mid-infrared (IR) and near-IR diffuse reflectance spectroscopy (DRIFT). Difference bands were observed in the 2650- to 2750-cm^{-1} region. This region coincides with the kaolinite-deuterated hydroxyl stretching region. Summation bands were observed in the near-IR spectra in the 4500- to 4650-cm^{-1} and in the 7050- to 7250-cm^{-1} region. Each of the spectral regions of the summation and difference bands is both kaolin polytype and sample dependent. It is proposed that each of these sets of bands arises from the combination of the hydroxyl stretching frequencies and the hydroxyl deformation frequencies and, to a lesser extent, the silicon-oxygen symmetric stretching vibration of the siloxane layer. Additional difference bands of very low intensity were also observed at 2930 and 2856 cm^{-1}. Combination bands were observed in all kaolinites at 2137 and 2227 cm^{-1}. Each of the 3 major combination spectral regions was composed of 5 component bands corresponding to the 4 IR active and the 1 Raman active kaolinite hydroxyl stretching frequencies. Combination bands were also observed at ~1932 and 1821 cm^{-1}.

Key Words—Combination Bands, Difference Bands, DRIFT, Kaolins, Kaolinites, Mid-Infrared, Near-Infrared, Raman.

INTRODUCTION

There are numerous techniques available to the clay scientist for obtaining molecular information. These techniques include both Raman and IR spectroscopy. Among the IR spectroscopic techniques, there are 1) the absorption (KBr) technique, 2) IR emission spectroscopy (IES), 3) the reflectance techniques, including diffuse and specular reflectance, 4) attenuated total reflectance (ATR), 5) IR microscopy and 6) photoacoustic Fourier transform IR (FTIR) spectroscopy (PAS). In particular, the selection of the technique depends on the particular problem at hand. For example IES is suitable for studying kaolinite dehydroxylation and thermal changes in kaolinites at elevated temperatures (Frost and Vassallo 1996). The pressing of a KBr pellet with clays may alter the spectrum through absorption or exchange of the K into the clay structure. ATR is useful for powders but is limited by the signal-to-noise ratio determined by the energy throughput. PAS is a nondestructive technique useful for handling clays but is limited by the number of samples that may be handled in a given period of time. Specular reflectance is not readily applicable to clay minerals, as the technique normally applies to flat, shiny polished surfaces, although specular IR reflectance studies have been used to study thermally treated Li and Cs montmorillonites (Karakassides et al. 1997). DRIFT is more applicable to powders but is limited to some extent by the Restrahlen effects where the particle size and the incident IR wavelengths create interference effects. Such effects are minimized by mixing the clay with KBr at the 5% level. The advantage of using the DRIFT technique is that it provides a rapid technique for analyzing samples without any interference through sample preparation. The DRIFT technique avoids the possibility of ion exchange of the K ion and non-randomly oriented samples. The technique is particularly useful where the Restrahlen effects are minimal. These effects appear toward the low-frequency region, normally below 1000 cm^{-1}. Thus, the DRIFT technique lends itself to the study of the hydroxyl stretching region of kaolinites where such effects are not observed. Also, the DRIFT technique is most suited to the near-IR region where the hydroxyl summation bands occur.

The vibrational spectroscopy of kaolins has attracted considerable interest due to its application to the kaolin structure. Hydroxyl bands are very sensitive probes for distinguishing between kaolin clay minerals and determining their structure (Frost 1997). FT Raman spectroscopy has already proven a very powerful technique in the study of kaolin minerals (Frost et al. 1993; Frost 1995). The assignment of the hydroxyl stretching bands remains under constant review, and differing viewpoints concerning the position and orientation of the hydroxyl groups exist (Giese 1988; Hess and Saunders 1992). Kaolinite, as with the other kaolin polytypes, contains 2 types of hydroxyl groups: 1) the outer hydroxyl groups, or so-called "inner surface hydroxyls", designated "OuOH" and 2) the inner hydroxyl groups, designated "InOH". The OuOH groups are situated in the outer upper, unshared plane,

† Permanent address: Department of Chemical and Metallurgical Engineering, Division of Inorganic Chemistry, Luleå University of Technology, SE-971 87 Luleå, Sweden.

whereas the InOH groups are located in the plane shared with the apical oxygens of the tetrahedral sheet. In an ordered sample such as the Georgia kaolinite (KGa-1), the 4 distinct IR bands are observed as follows: the 3 higher-frequency vibrations (ν_1, ν_2, ν_3) are assigned to the 3 outer (OuOH) hydroxyls and the ν_5 band at 3620 cm^{-1} to the inner hydroxyl (InOH) (Farmer 1974; Frost and van der Gaast 1997). The fourth band at 3685 cm^{-1} (ν_4) is Raman active and IR inactive. The commonly accepted view is that the ν_1 and ν_2 bands are the coupled antisymmetric and symmetric vibrations (Brindley et al. 1986; Michaelian 1986). The coupling of these bands means that overtones and combination bands may also be observed. The assignment of the ν_3 band is open to question but the suggestion has been made that the band is due to symmetry reduction of the OuOH hydroxyl (Farmer and Russell 1964).

Kaolinites may be classified according to the ratio of the 2 OuOH hydroxyls at 3685 and 3695 cm^{-1} (Frost and van der Gaast 1997). The intensity of the 3650- and 3670-cm^{-1} bands was found to vary concomitantly with the 3685- and 3695-cm^{-1} bands, respectively. It was hypothesized that the 3650-cm^{-1} band is the out-of-phase counterpart of the in-phase vibration at 3685 cm^{-1} and the 3670-cm^{-1} band is the out-of-phase analogue of the in-phase vibration at 3695 cm^{-1}. Linear relationships were found between the intensities of these in-phase and out-of-phase vibrations. Linear combinations of these vibrational modes mean that combination bands involving the Raman active modes will also be possible. A hypothesis based on theoretical studies suggested a model of hydrogen bonding to explain the reason for 2 OuOH bands at 3695 (ν_1) and 3685 (ν_4) cm^{-1}. This hypothesis was based on models for hydrogen bonding between the inner surface hydroxyls of one layer and the siloxane units of the next adjacent kaolinite layer. The 3685-cm^{-1} band is IR inactive and Raman active, although in some very highly ordered kaolinites a band component may be observed in this position. In the near-IR spectra, combination bands may also arise from this type of vibration. Other hydroxyl bands are observed at 915 and 935 cm^{-1}. These bands are attributed to the hydroxyl deformation modes of the inner hydroxyl and the inner surface hydroxyl modes, respectively (Frost 1998). Such bands may also couple with other bands to give overtone and combination bands in the near-IR region.

While IR spectroscopy has been extensively used for the study of clay minerals, many of the newer techniques have yet to be applied to the study of clay mineral structures (Lazarev 1972; Farmer 1974). For example, IES has been used to a limited extent to study dehydroxylation of kaolin polymorphs (Frost and Vassallo 1996). IR spectroscopy has been used extensively for the characterization of kaolinites, particularly with respect to the determination of order, crystallinity and energy of cohesion between kaolinite sheets (Cases et al. 1992; Cruz-Cumplido et al. 1992; Yvon et al. 1992). Near-IR spectroscopy has also been used for a considerable length of time and, more recently, for the study of the kaolinite clay minerals (Matsunaga and Uwasawa 1993; Tanabe et al. 1994). Indeed, remote sensing has identified minerals using near-IR spectroscopy (Hunt and Ashley 1979; Hunt and Hall 1981). Near-FTIR has been used for the studies of structural iron in kaolinites (Delineau et al. 1994), the quantitative analysis of kaolin mixtures (Crowley and Vergo 1988), the presence of kaolinite in altered rocks (Hunt and Hall 1981) and the study of the deuteration of kaolinite (Michaelian et al. 1987; Johansson et al. 1998). Two IR absorption band regions were observed at 4465 and 7025 cm^{-1}. Explanation of the origin of these bands was limited (Hunt et al. 1973) and direct proof of the origin of the bands was not given. Difference bands have not been reported. The objective of this research is to report the FTIR hydroxyl summation and difference bands of kaolinite and to determine the origin of these bands. Furthermore, this work reports the overlap of the kaolinite difference bands with the deuterol stretching bands of kaolinite.

EXPERIMENTAL

Clay Mineral Samples

Clay minerals were obtained from The Clay Minerals Society Repository and from the Australian Commonwealth Scientific and Industrial Research Organisation, Glen Osmond, South Australia. Minerals were collected from a number of Australian mineral deposits. Samples were analyzed for phase purity using X-ray diffraction (XRD) techniques before DRIFT spectroscopic analysis. Table 1 shows the origin and source of the kaolinites and other kaolin polytypes.

XRD of powder patterns of the kaolinites was obtained using a Philips PW 1050 X-ray diffractometer using Co$K\alpha$ radiation operating at 35 kV and 40 mA. A 1° divergence and scatter slit were combined with a normal focus Co tube at 6° takeoff and a 0.2-mm receiving slit. The samples were measured in stepscan mode from 2.0 °2θ with steps of 0.05° up to 40 °2θ and a counting time of 2 s. XRD was used to determine the Hinckley Index of the kaolinites, which was used as a measure of the defect structures of the kaolinite (Hinckley 1963). The Hinckley Index of kaolinite crystallinity is determined by measuring the ratio of the intensities of the 110 and 111 peaks above a line drawn from the trough between the 020 to 110 peaks to the background beyond the 110 peak. These Hinckley indices are shown in Table 1. Kaolinites were analyzed for chemical composition using inductively coupled plasma-atomic emission spectroscopy (ICP-AES) techniques. Deuteration of the Amazonian

https://doi.org/10.1346/CCMN.1998.0460411 Published online by Cambridge University Press

Table 1. Table of kaolinites, their origin and the source of supply.

Kaolinite polymorph	Hinckley Index	Locality	Origin
Kaolinite #9	1.35	Mesa Alta, Mexico	Wards Natural Science establishment
Kaolinite	0.42	Amazon	Brazil
Kaolinite	1.38	Lal-lal, Victoria, Australia	M. Stielow Enterprises Pty Ltd.
Kaolinite	0.25	Williamstown, South Australia	Commercial Minerals Pty Ltd.
Kaolinite	1.4	Birdwood, South Australia	Commercial Minerals Pty Ltd.
Kaolinite	0.12	Weipa 1	Comalco Pty Ltd.
Kaolinite	0.20	Weipa 2	Comalco Pty Ltd.
Kaolinite	0.5	Pittong	English China Clays Pty Ltd.
Kaolinite	0.65	Eyres Peninsula, South Australia	Commercial Minerals Pty Ltd.
Kaolinite	0.1	Mt. Hope (South Australia)	Commercial Minerals Pty Ltd.
Halloysite	—	New Zealand	New Zealand China Clays Pty Ltd.
Halloysite	—	Eureka, Utah	Clay Mineral Society Standard
Dickite	—	San Juanito, Mexico	Wards Natural Science establishment

kaolinite was undertaken by mixing the dried kaolinite in deuterium oxide in a sealed vessel at 60 °C for 5 weeks. The extent of deuteration was determined by the decrease in intensity of the hydroxyl bands.

DRIFT Spectroscopy

Drift spectra were obtained using a Perkin-Elmer FTIR spectrometer (2000) equipped with a triglycline sulfate (TGS) detector. Spectra were recorded by accumulating 128 scans at 8 cm^{-1} resolution using a mirror velocity of 0.2 cm/s for the near-IR and 1024 scans at 4 cm^{-1} resolution and a mirror velocity of 0.3 cm/s in the mid-IR. Approximately 5% kaolin was dispersed in oven-dried spectroscopic grade KBr with a refractive index of 1.559 and a particle size of 5–20 μm. Background KBr spectra were obtained and spectra ratioed to the background. A series of kaolinites, halloysites and dickites of different crystallinity and particle size were analyzed. Spectra were recorded in both the mid-IR and near-IR regions. The spectra were transformed using the Kubelka-Munk algorithm to provide spectra for comparison with absorption spectra. The spectral manipulations of baseline adjustment, smoothing and normalization were performed using the Spectracalc software package GRAMS (Galactic Industries Corporation, New Hampshire). Band component analysis was carried out using the peakfit software by Jandel Scientific. Lorentz-Gauss cross-product functions were used throughout and peak fitting carried out until squared correlation coefficients with r^2 greater than 0.995 were obtained.

RESULTS

The IR spectra of the kaolinite polymorphs are complicated by the presence of combination bands, which are obvious in the near-IR spectra but less obvious in the mid-IR. Three major sets of bands were observed in regions around ~2700, 4600 and 7050 cm^{-1}. Figure 1 illustrates the 2700-cm^{-1} region (difference region 1), Figure 2 the 4500-cm^{-1} region (summation region 1) and Figure 3 the 7050-cm^{-1} region (summation region 2) for the kaolin polytypes. The differences in the spectra may be correlated to the differences in the hydroxyl stretching region of the kaolin polytypes (Hunt et al. 1973; Lindberg and Snyder 1972). Each kaolin has its own characteristic near-IR spectrum. The near-IR spectrum of water was observed in this region at 5263 cm^{-1} (1.9 μm). The near-IR spectrum of adsorbed water is absent in the spectra reported in this research. Hunt et al. (1973) reported that the kaolin polytypes had a single prominent band at 4545 cm^{-1} (2.2 μm). This band was characteristic of 2-layer dioctahedral minerals. Bands were also observed at 6756 cm^{-1} (1.48 μm) and 6993 cm^{-1} (1.43 μm). Previous work has not reported difference bands in the mid-IR spectra of kaolinites (Hunt et al. 1973; Brindley et al. 1986). Figure 1 illustrates the DRIFT spectra of the hydroxyl difference bands observed. It may be clearly observed that difference bands are common to all of the kaolinites studied in this work.

In the DRIFT spectra reported in this work, more clearly resolved bands were observed. For the first summation region centered on 4545 cm^{-1} (2.2 μm) (Figure 2), the 2 halloysites have slightly different spectra with differences in the 4625-cm^{-1} region. This difference may be attributed to the amount of water in the halloysite structure. Previous studies reported broad unresolved spectra for halloysites that were dependent on the water content of the halloysite (Hunt et al. 1973). The kaolinite, in this example a highly ordered kaolinite from South Australia, shows a prominent band at 4527 cm^{-1} together with bands at 4558, 4610 and 4632 cm^{-1}. The dickite spectrum shows a very different spectrum with a pronounced band at 4590 cm^{-1}. For the second summation region centered at 6995 cm^{-1} (1.43 μm), the 2 halloysites show weak but similar spectra (Figure 3). The spectral pattern is quite complex with the most prominent band observed at 7067 cm^{-1} (1.415 μm). Kaolinites show better-resolved bands in this region with 2 features at 7067 and 7168 cm^{-1}. Dickites show better resolution with 2 prominent bands at 7067 and 7225 cm^{-1}. Previous work showed 2 well-resolved bands for dickite at 1.43 (6993 cm^{-1}) and 1.48 μm (6756 cm^{-1}) which are at frequencies somewhat less than observed in this work (Hunt and Ashley 1979; Hunt et al. 1973). The spec-

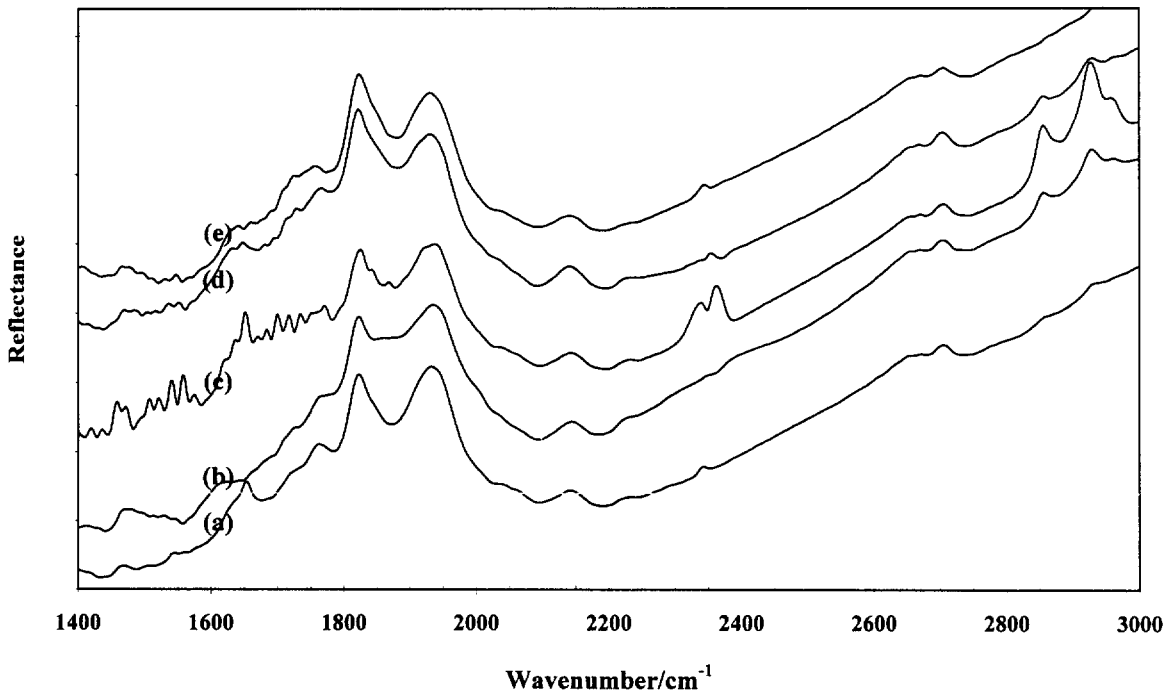

Figure 1. DRIFT spectra of the hydroxyl difference bands in the 1400- to 3000-cm^{-1} region of kaolinites from (a) Birdwood (South Australia), (b) Mesa Alta (Mexico), (c) Lal-lal (Victoria, Australia), (d) Eyre Peninsula (South Australia) and (e) Amazon (Brazil).

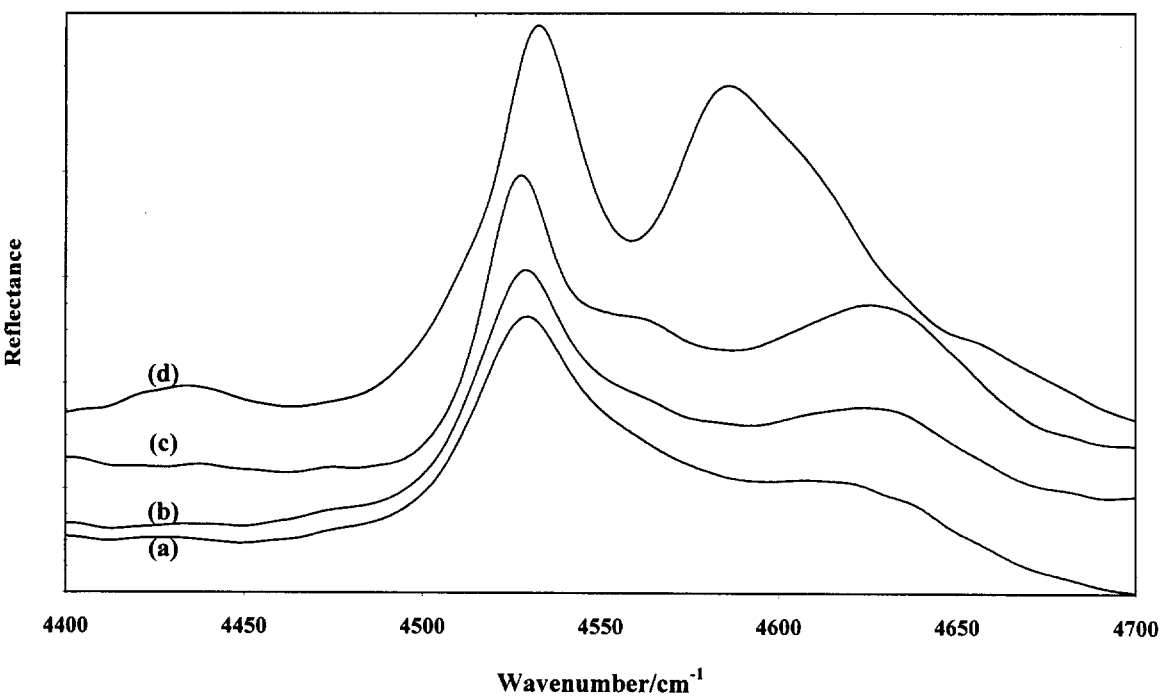

Figure 2. DRIFT spectra of the hydroxyl summation bands in the 4400- to 4700-cm^{-1} region of (a) halloysite (Eureka, Utah), (b) halloysite (NZ), (c) kaolinite (Birdwood, Australia) and (d) dickite (San Juanito, Mexico).

https://doi.org/10.1346/CCMN.1998.0460411 Published online by Cambridge University Press

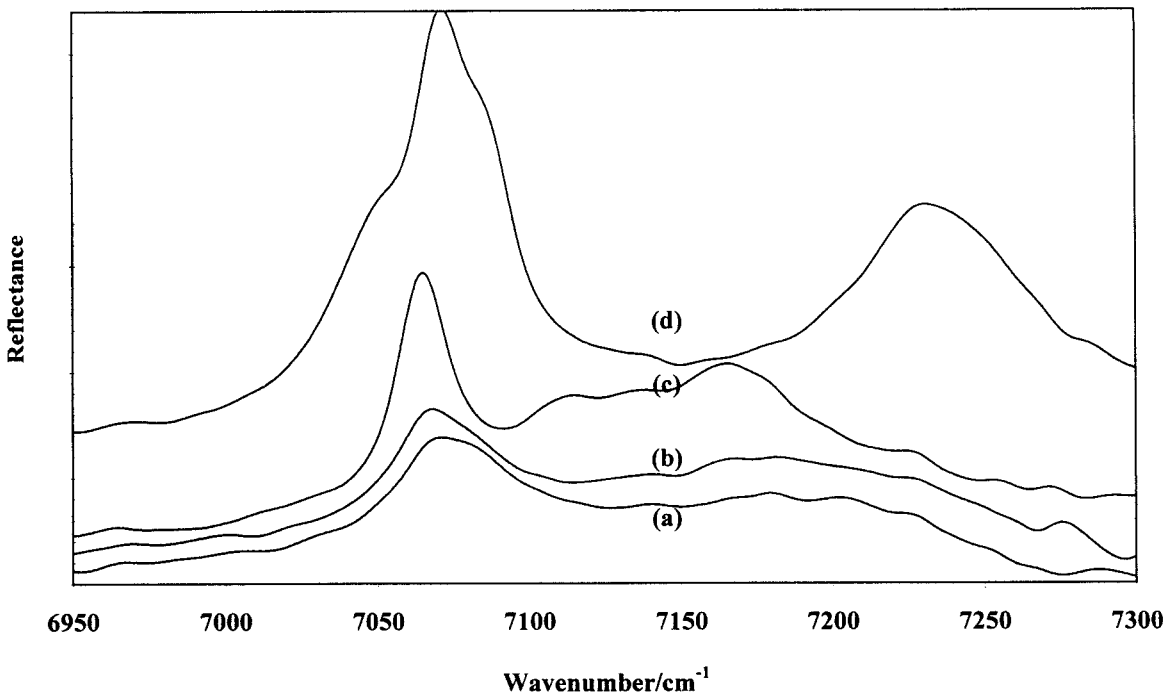

Figure 3. DRIFT spectra of the hydroxyl summation bands in the 6950- to 7900-cm^{-1} region of (a) halloysite (USA), (b) halloysite (NZ), (c) kaolinite (Birdwood, Australia) and (d) dickite (San Juanito, Mexico).

trum of summation region 1 for the kaolinite shows a strong resemblance to that of its hydroxyl stretching region. The dickite spectrum is very different, showing considerable complexity. Two well-resolved bands are observed.

Figures 4, 5 and 6 show the spectra for a series of kaolinites with different defect structures. In terms of relative intensities, the bands in the 4500- to 4650-cm^{-1} region are approximately 1 tenth of the intensity of the hydroxyl stretching bands between 3620 and 3695 cm^{-1} (Figure 7 and Table 2). The intensities of the set of bands between 7050 and 7200 cm^{-1} are approximately 0.75 of the intensity of the 4500- to 4650-cm^{-1} bands. The spectra for kaolinites show some resolution of component bands with the kaolinites characterized by the band at 4525 cm^{-1}. Each set of bands shows a constant pattern for each of the spectral regions and each spectral region may be decomposed into 4 major component bands (Figures 8 and 9). Table 2 reports the frequencies of these component bands. In the 4500- to 4700-cm^{-1} region, 5 bands were observed with approximately equal intensities, as determined by band areas at 4527, 4558, 4610 and 4632 cm^{-1} with a less intense band at 4649 cm^{-1}. The 4527-cm^{-1} band is the most prominent in this spectral region. In the 7050- to 7200-cm^{-1} region, 4 intense bands were observed at 7067, 7118, 7168 and 7182 cm^{-1} with a smaller component at 7156 cm^{-1}.

DISCUSSION

The question arises as to the reason for the observed combination bands. For kaolinite, there are several possibilities. It was first considered that the bands in the 4500- to 4700-cm^{-1} region arise from addition of the hydroxyl stretching frequencies and the silicon oxygen stretching frequency. One possibility is that the 4527-cm^{-1} band is the addition of the 3621 + 1021 cm^{-1} bands. Such a combination arises from the addition of the inner surface hydroxyl stretching frequency and the Si-O stretching frequency of the siloxane layer. The observed band at 4527 cm^{-1} is some 120 cm^{-1} less than the expected frequency of 4642 cm^{-1}. This is then an unlikely combination of 2 vibrational frequencies even though the hydroxyl symmetric stretch and the siloxane Si-O stretching frequency are coupled through hydrogen bonding. It has been suggested that the 4527-cm^{-1} region can be attributed to the combination of the hydroxyl stretching frequency and the low-frequency vibrational modes (Hunt et al. 1973). A second possibility is the combination of the hydroxyl stretching frequencies and the hydroxyl deformation modes. The sharp band at 4527 cm^{-1} arises from the addition of the hydroxyl stretching 3621-cm^{-1} band and the hydroxyl deformation band at 915 cm^{-1} (Frost 1998). This would give an addition of 4536 cm^{-1}, which is closer to the observed frequency of 4527 cm^{-1}. Thus, it would appear that the hydroxyl

https://doi.org/10.1346/CCMN.1998.0460411 Published online by Cambridge University Press

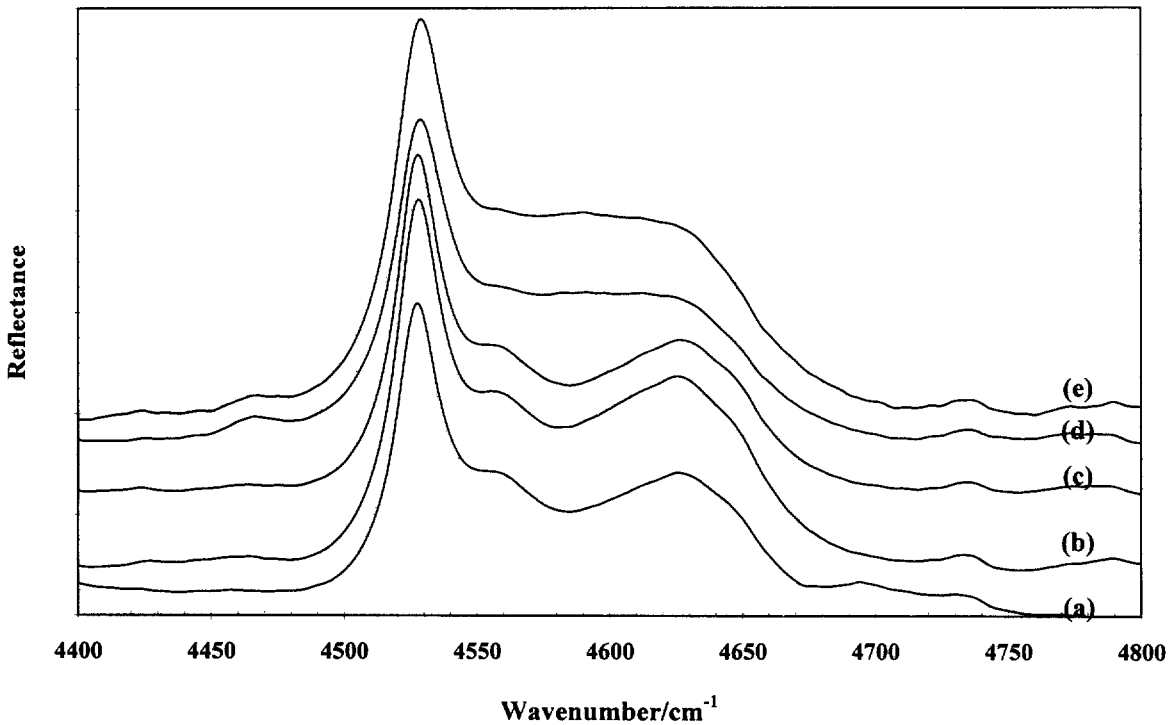

Figure 4. DRIFT spectra of the hydroxyl summation bands in the 4400- to 4800-cm^{-1} region of kaolinites from (a) Mt. Hope (South Australia), (b) Lal-lal (Victoria, Australia), (c) Pittong (Victoria, South Australia), (d) Weipa (Queensland, Australia) and (e) Weipa (Queensland, Australia).

stretching frequency is combining with the hydroxyl deformation frequency to give rise to the combination band at 4527 cm^{-1}. Similarly, it is proposed that the component bands at 4558 cm^{-1} arise from the combination of the hydroxyl stretching frequency at 3652 cm^{-1} attributed to the inner surface hydroxyl bands and the hydroxyl deformation vibration at 915 cm^{-1}. The 2 bands at 4610 and 4632 cm^{-1} arise from the combination of the 3670- and 3697-cm^{-1} with the hydroxyl deformation vibration of the inner surface hydroxyl groups. The combination bands therefore originate from the combination of bands from vibrational modes of the same group; that is, the combination of the hydroxyl stretching frequency and the hydroxyl deformation frequency arising from the same hydroxyl groups. Thus, specific vibrational modes arising from the mixing of modes from the same hydroxyl group combine to give the spectral profile in the 4500- to 4650-cm^{-1} region. A very weak band common to all kaolinites studied was observed at ~4195 cm^{-1} (2.38 μm).

The bands in the 7050- to 7200-cm^{-1} region in all probability arise from the doubling of the hydroxyl stretching frequencies. If we take the inner hydroxyl stretching frequency at 3621 cm^{-1} and double this number, the value of 7242 cm^{-1} is obtained, which is of the order of 175 cm^{-1} greater than the observed frequency of 7067 cm^{-1}. The IR symmetric stretching vibration of the inner hydroxyl at 3621 cm^{-1} has a bandwidth of 18 cm^{-1}. The bandwidth of the 7067-cm^{-1} band is 21.6 cm^{-1}. These bandwidths assist in the confirmation that the 7067-cm^{-1} band is the duplication in frequency of the 3621-cm^{-1} band. If the frequency of 3697 cm^{-1} is doubled, a value of 7394 cm^{-1} is obtained, which is 212 cm^{-1} greater than the observed frequency of 7182 cm^{-1}. If the value of 3670 cm^{-1} is doubled, then a value of 7340 cm^{-1} is obtained, which is 172 cm^{-1} greater than the observed frequency of 7168 cm^{-1}. It is considered that the doubling of the 3652-cm^{-1} band does not occur. The 3652-cm^{-1} band has been described as an out-of-phase vibration and it is unlikely that out-of-phase vibrational modes would combine to give overtones (Frost and van der Gaast 1997). If it does, then the intensity of the band is too weak to observe. One way of describing the IR bands at 3652, 3670 and 3697 cm^{-1} is to attribute the 3697-cm^{-1} band as an in-phase vibration and the bands at 3652 and 3670 cm^{-1} as out-of-phase vibrations (Frost and Vassallo 1996; Frost and Van der Gaast 1997). If this is the correct description of these latter 2 bands, then it is unlikely that out-of-phase vibrations would couple to give bands in the 7050- to 7200-cm^{-1} region. Another possibility is that the near-IR band at 7050 cm^{-1} is due to the combination of a

https://doi.org/10.1346/CCMN.1998.0460411 Published online by Cambridge University Press

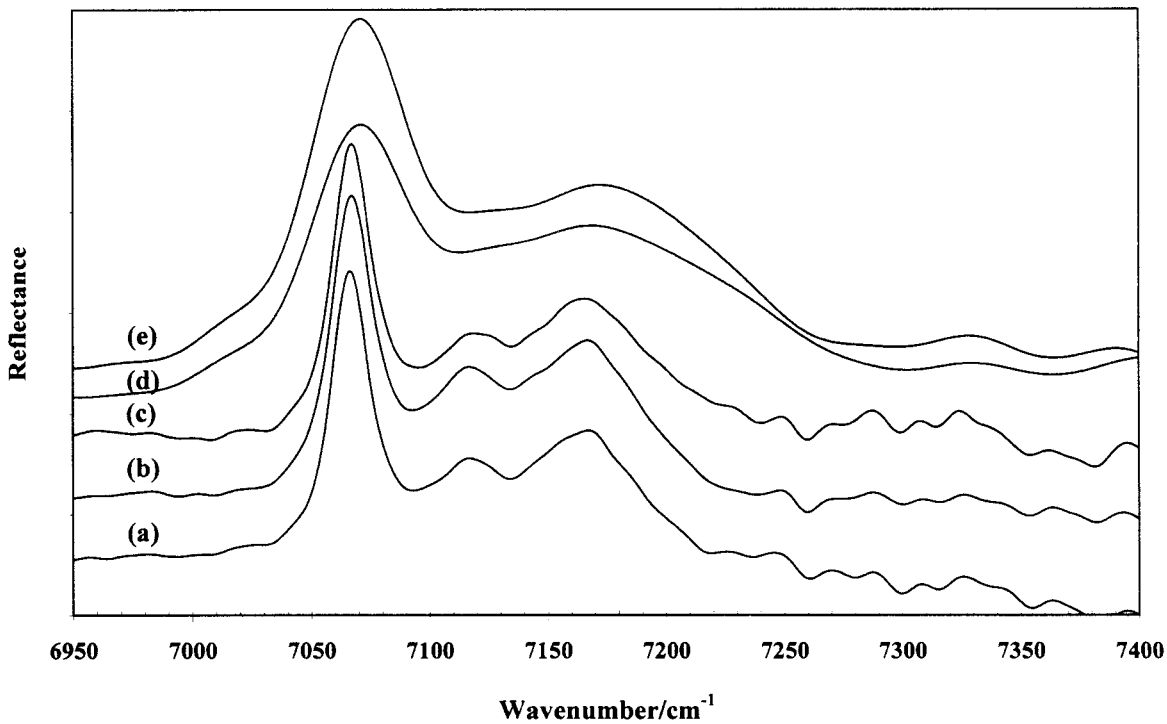

Figure 5. DRIFT spectra of the hydroxyl summation bands in the 6950- to 7400-cm^{-1} region of (a) Mt. Hope (South Australia), (b) Lal-lal (Victoria, Australia), (c) Pittong (Australia), (d) Weipa (Queensland, Australia) and (e) Weipa (Queensland, Australia).

Raman active mode and an IR active mode. For example, the bands in the 7050-cm^{-1} region have differences of 7156 − 3652, 7168 − 3670 and 7182 − 3697 cm^{-1}, which are 3504, 3498 and 3485 cm^{-1}, respectively. The constancy of these differences could then result from the combination of a single Raman mode and the various IR modes.

The bands observed in the 2650- to 2730-cm^{-1} region (Table 2) are attributed to difference bands based on the subtraction of specific frequencies from the hydroxyl stretching frequencies. These bands are centered around 2690 cm^{-1} with 2 major peaks at 2699 and 2709 cm^{-1} and 2 peaks of less intensity at 2671 and 2655 cm^{-1}. This spectral region is complex and band fitting does not fit this region well (Figure 10). Nevertheless, 2 major bands were observed at 2698.5 and 2709.5 cm^{-1} with about equal bandwidths of 15.5 cm^{-1}. It is possible that the 2709.5-cm^{-1} band arises from the coupling of the 3620- and 915-cm^{-1} frequencies. The difference in these 2 frequencies is 2705 cm^{-1}, which corresponds well with the observed frequency of 2709.5 cm^{-1}. The 3620-cm^{-1} Raman band resolves into 2 bands at 3617 and 3628 cm^{-1} at liquid nitrogen temperatures, so consequently the 3620-cm^{-1} band consists of 2 overlapping coincident bands that only become resolved at low temperatures. The coupling with the 915-cm^{-1} band may also cause the resolution of these 2 bands in the mid-IR difference spectra. The band at 2671 cm^{-1} is of medium intensity for this set of bands. One possibility is that the band arises from the difference between the 3697- and 1020-cm^{-1} bands. The complexity of this spectral region may be attributed to the subtraction of both the hydroxyl deformation frequencies and the siloxane Si-O frequencies from the hydroxyl stretching frequencies. In a simple analysis, there are 5 hydroxyl stretching frequencies (4 in the FTIR and 5 in the Raman) that could combine with 2 hydroxyl deformation frequencies and several siloxane Si-O stretching frequencies. This would result in some 20 possible combinations, which makes the difference spectra complex.

When kaolinite is deuterated, the deuterol stretching frequencies occur in the 2660- to 2740-cm^{-1} region (Table 2). For the kaolinite from Amazon, 5 deuterol bands were observed at 2672, 2680, 2698, 2721 and 2732 cm^{-1} for the partially deuterated kaolinite (Figure 11). It is obvious that the deuterol spectral region of the deuterated kaolinite overlaps with the difference bands of kaolinite. The 2705-cm^{-1} band makes up 50% of the total band intensity of the difference band profile of the untreated kaolinite. This band profile coincides exactly with the deuterol band profile. This makes the analysis of the spectral region of the deuterated kaolinite difficult, as both sets of bands occur

https://doi.org/10.1346/CCMN.1998.0460411 Published online by Cambridge University Press

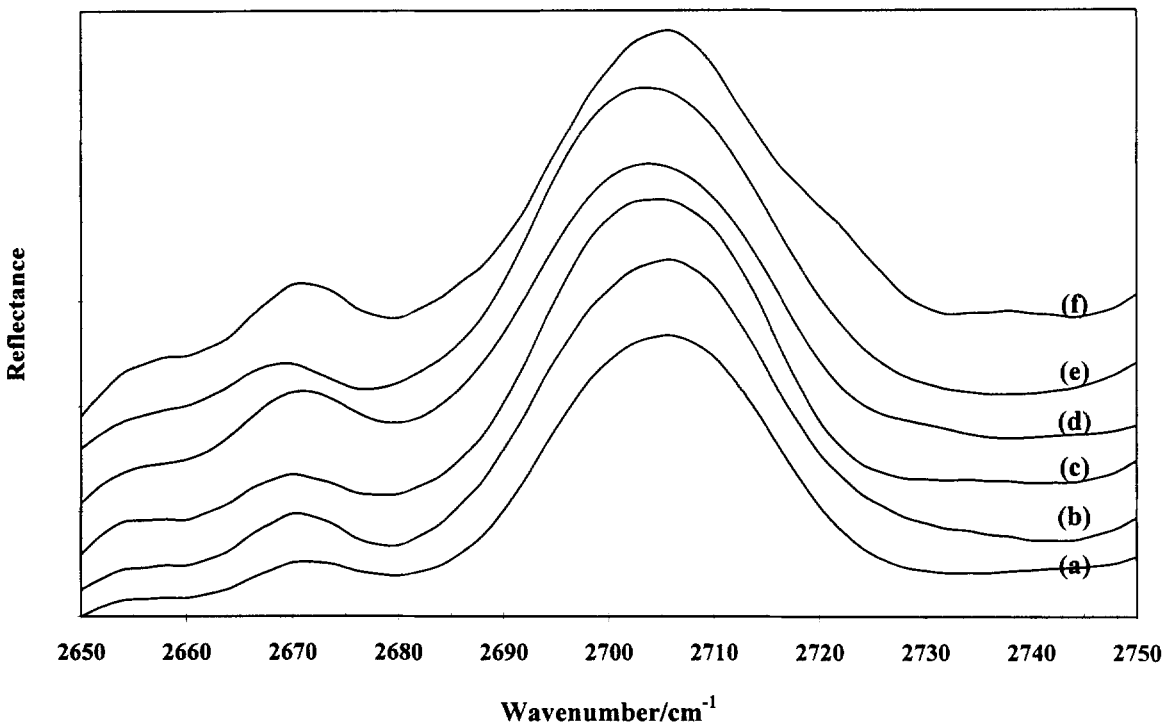

Figure 6. DRIFT spectra of the difference bands of kaolinite in the 2650- to 2750-cm^{-1} region of kaolinites from (a) Birdwood (South Australia), (b) Mesa Alta (Mexico), (c) Lal-lal (Victoria, Australia), (d) Mount Hope (South Australia), (e) Eyre Peninsula (South Australia) and (f) Amazon (Brazil).

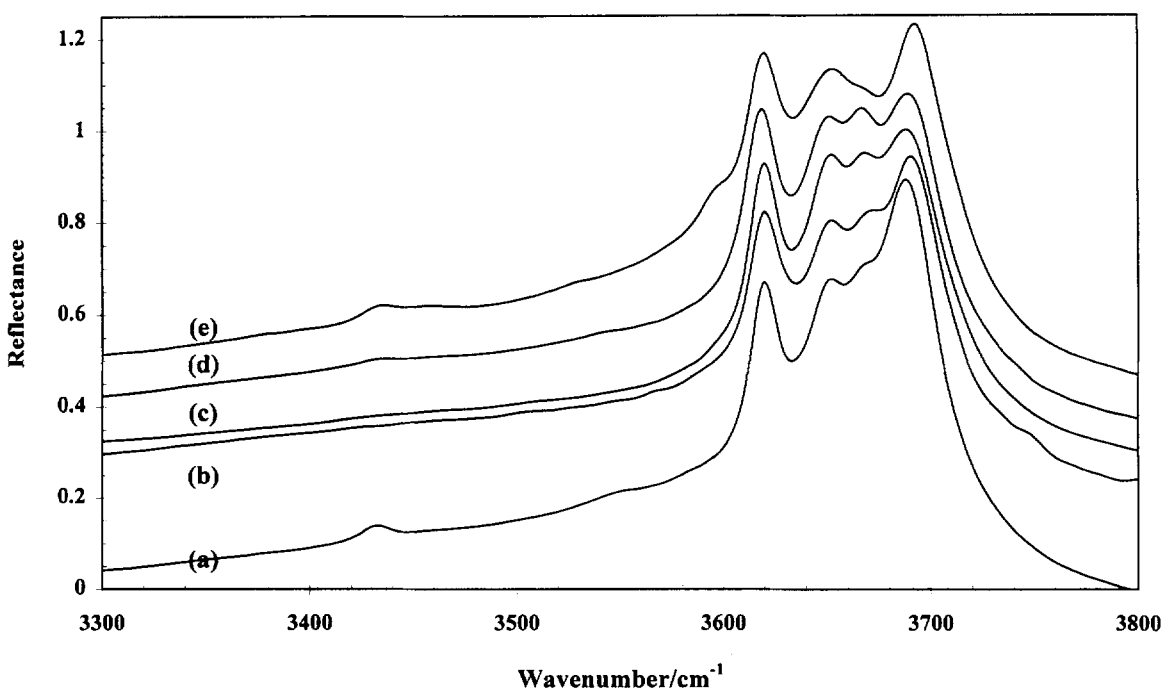

Figure 7. DRIFT spectra of the hydroxyl stretching of kaolinites in the 3300- to 3700-cm^{-1} region from (a) Birdwood (South Australia), (b) Mesa Alta (Mexico), (c) Lal-lal (Victoria, Australia), (d) Eyre Peninsula (South Australia) and (e) Amazon (Brazil).

https://doi.org/10.1346/CCMN.1998.0460411 Published online by Cambridge University Press

Table 2. Band component analyses of the DRIFT spectra of Amazonian kaolinite.

Deuterol stretching region 2700-cm^{-1} region	Hydroxyl stretching region	4500-cm^{-1} region	7050-cm^{-1} region	2700-cm^{-1} region
2672	3621.5	4527	7067	2655
—	3637	4558	7118	2671
2698	3652	4610	7156	2698.5
2721	3670	4632	7168	2703
2732	3697	4649	7182	2709.5

at similar frequencies, particularly for partially deuterated kaolinites. There is, however, a considerable difference in intensities. The deuterol bands are about 3 times as intense as the difference bands. Deuterol difference bands were not observed. It was considered that these bands were of extremely low intensity. Additional kaolinite difference bands of very low intensity were also observed at 2930 and 2856 cm^{-1} (Figure 1). Bands that involve the hydroxyl group have been identified in Raman spectroscopy at 141 and 230 cm^{-1} (Frost et al. 1993; Frost 1995). Further bands have been observed at 670, 707, 754 and 789 cm^{-1} and were attributed to hydroxyl translation vibrations involving the flexing of the kaolinite lattice (Frost et al. 1993; Frost 1995). The difference between the 3620- and 670-cm^{-1} bands is 2950 cm^{-1}, which is close to the observed band at 2930 cm^{-1}. An alternative is the difference between the 3695-cm^{-1} band and the 754-cm^{-1} band of 2944 cm^{-1}. Thus, it is probable that the bands observed at 2930 and 2856 cm^{-1} are the difference between the hydroxyl stretching vibrational frequency and the hydroxyl translation frequency. Combination bands were also observed in all kaolinites at 2137 and 2227 cm^{-1} (Figure 1). It is not known which combination of bands gives rise to these frequencies, but it is probable that the frequencies are overtones of low-frequency vibrations such as the doubling of the Si-O stretching frequency at 1020 cm^{-1}. Deuteration of the kaolinite resulted in the removal of these combination bands. Bands were also observed at 1932 and 1821 cm^{-1}. These bands are attributed to the combination of the Si-O stretching (1020 cm^{-1}) and hydroxyl deformation frequencies (915 cm^{-1}) and the doubling of the hydroxyl deformation frequency at 915 cm^{-1}, respectively.

CONCLUSIONS

Kaolinites have been studied using near-IR and mid-IR spectroscopy. Both summation and difference bands were observed, and attempts at rationalizing the origin of these combination bands were made. Summation bands were observed in the near-IR spectra in the region from 4500 to 4650 cm^{-1} and in the 7050- to 7250-cm^{-1} region. Difference bands were observed

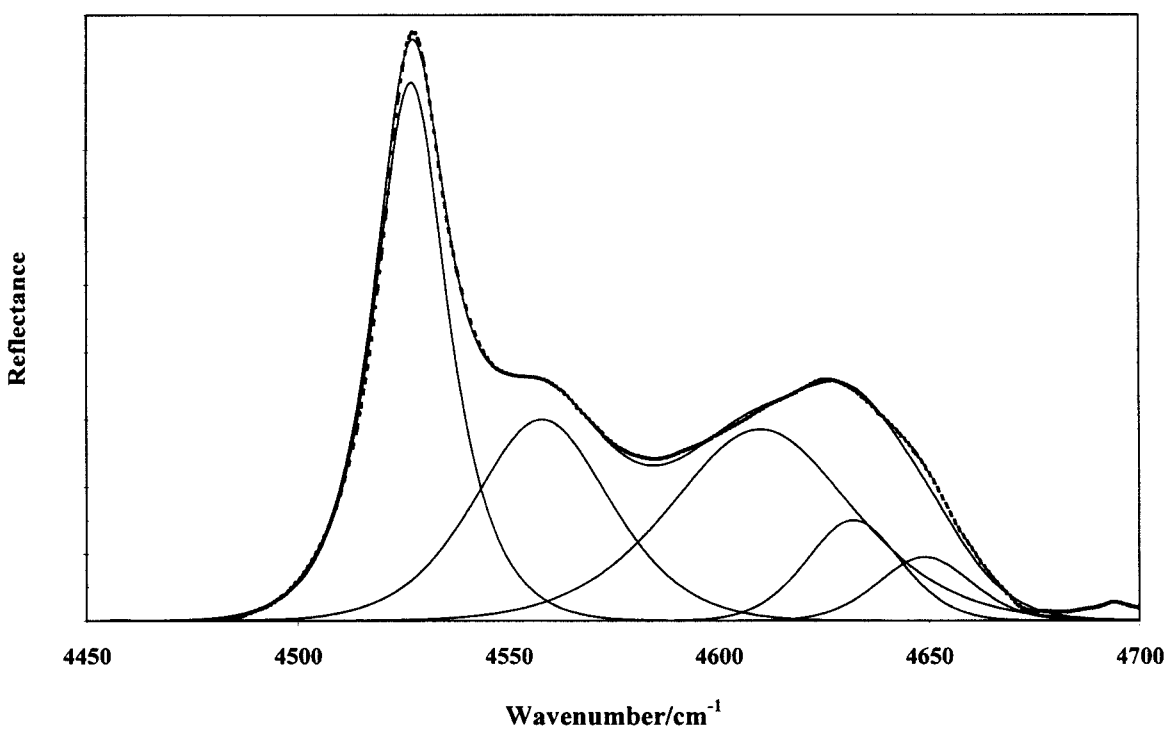

Figure 8. Band component analysis of the hydroxyl bands of the DRIFT spectra of Amazonian kaolinite in the 4450- to 4700-cm^{-1} region.

https://doi.org/10.1346/CCMN.1998.0460411 Published online by Cambridge University Press

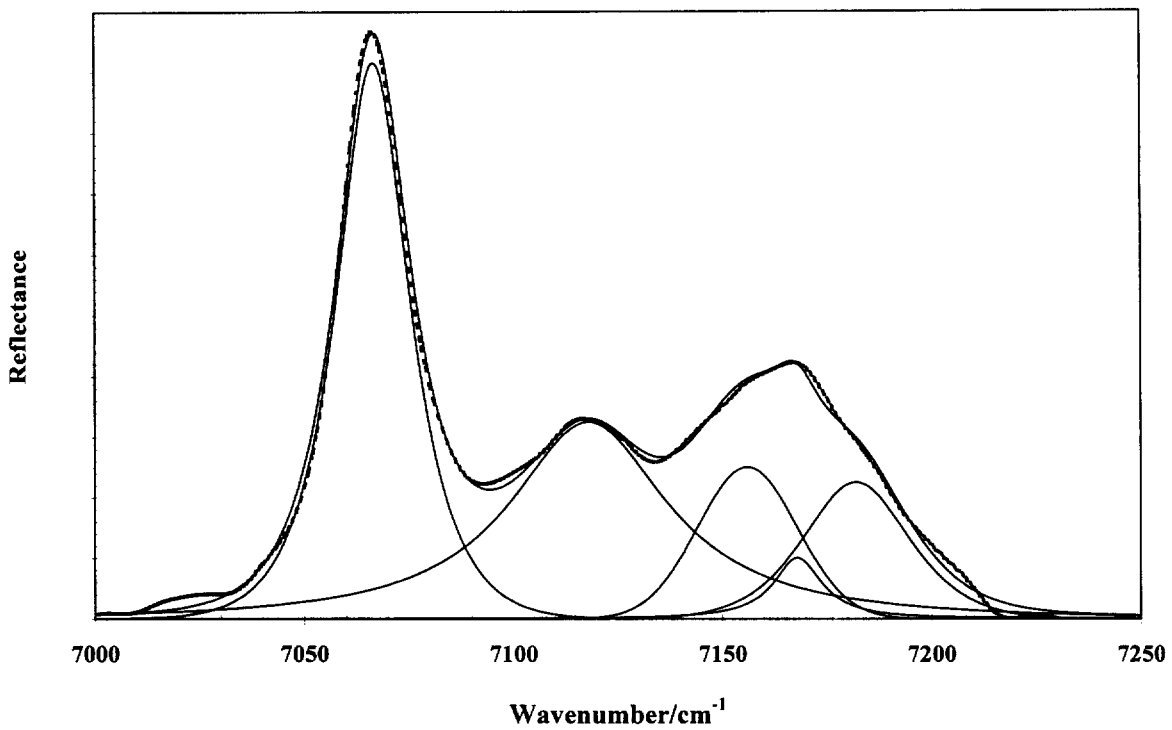

Figure 9. Band component analysis of the hydroxyl bands of the DRIFT spectra of Amazonian kaolinite in the 7000- to 7250-cm^{-1} region.

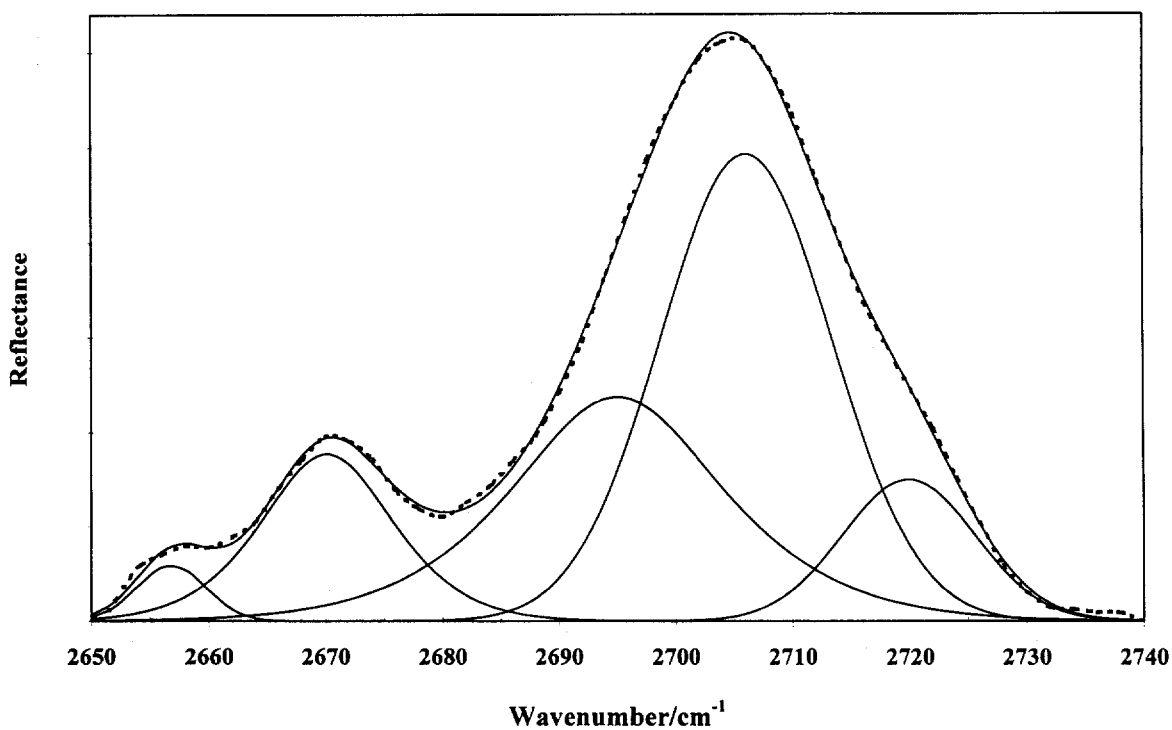

Figure 10. Band component analysis of the hydroxyl bands of the DRIFT spectra of Amazonian kaolinite in the 2650- to 2740-cm^{-1} region.

https://doi.org/10.1346/CCMN.1998.0460411 Published online by Cambridge University Press

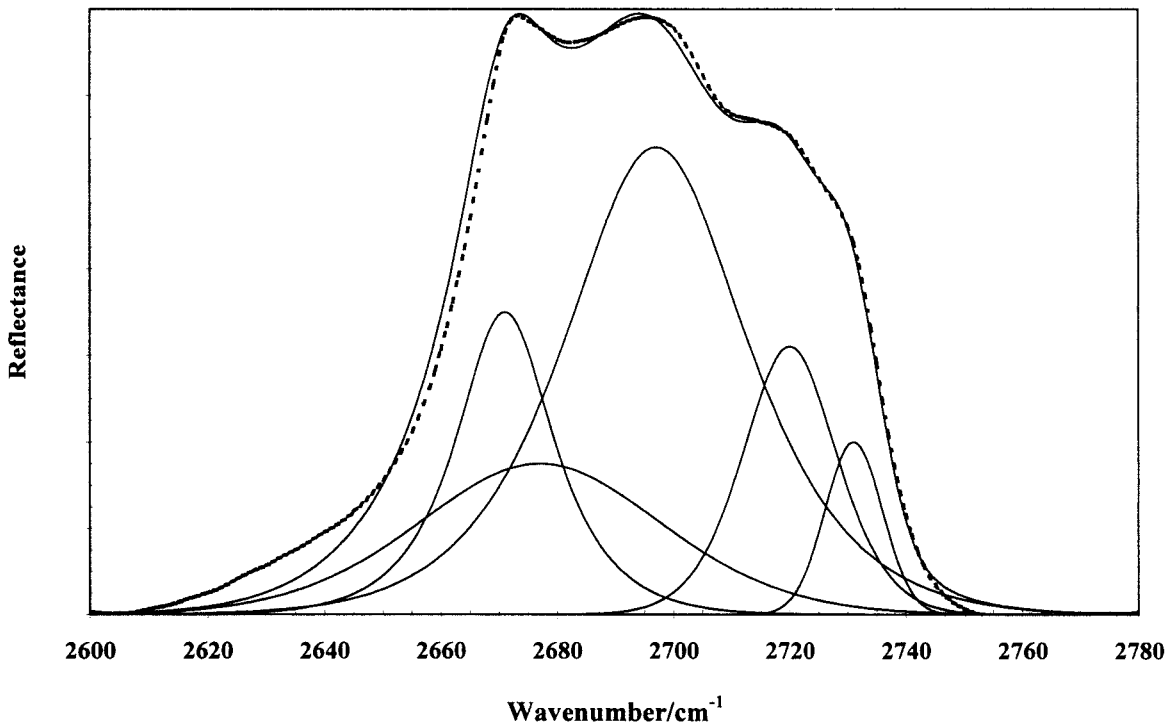

Figure 11. Band component analysis of the deuterol bands of the DRIFT spectra of Amazonian kaolinite in the 2600- to 2780-cm^{-1} region.

in the 2650- to 2750-cm^{-1} region. This latter region coincides with the kaolinite deuteration-stretching region. Each of the spectral regions of the summation and difference bands is both polymorph and sample dependent. It is proposed that each of these bands arises from the combination of the hydroxyl stretching frequencies and the other hydroxyl vibrations such as the deformation modes and the silicon-oxygen symmetric stretching vibration of the siloxane layer. Additional difference bands of very low intensity were also observed at 2930 and 2856 cm^{-1}. Combination bands were also observed in all kaolinites at 2137 and 2227 cm^{-1} and also at 1932 and 1821 cm^{-1}.

Importantly, care must be exercised in the study of kaolin spectra when low-intensity bands are found as occurs with deuteration and intercalation. Furthermore, while near-IR is used for the identification of the presence of kaolins, care should be taken if further interpretation is required. Certainly DRIFT spectroscopy in both the mid-IR and near-IR lends itself to the study of kaolins.

ACKNOWLEDGMENTS

The financial support of the Queensland University of Technology Centre for Instrumental and Developmental Chemistry is gratefully acknowledged. L. Barnes, chief geologist of Commercial Minerals, is also thanked for supply of several Australian kaolinites. The authors wish to thank J. M. Cases and T. Kloprogge for useful and constructive comments.

REFERENCES

Brindley GW, Chih-Chun K, Harrison JL, Lipsiscas M, Raythatha R. 1986. Relation between the structural disorder and other characteristics of kaolinites and dickites. Clays Clay Miner 34:233–249.

Cases JM, Lietard O, Yvon J, Delon JF. 1992. Étude des propriétés cristallochimiques, morphologiques, superficielles de kaolinites désordonnées. Bull Mineral 105:439–455.

Crowley JK, Vergo N. 1988. Near-infrared reflectance spectra of mixtures of kaolin-group minerals: Use in clay mineral studies. Clays Clay Miner 36:310–16.

Cruz-Cumplido M, Sow C, Fripiat JJ. 1992. Spectre infrarouge des hydroxyles, cristallinité et énergie de cohésion des kaolins. Bull Mineral 105:493–498.

Delineau T, Allard T, Muller J, Barres V. 1994. FTIR reflectance vs. EPR studies of structural iron in kaolinites. Clays Clay Miner 42:308–320.

Farmer VC. 1974. The layer silicates. In: Farmer VC, editor. The Infrared spectra of minerals. London: Mineral. Soc p 331–363.

Farmer VC, Russell JD. 1964. The infrared spectra of layered silicates. Spectrochim Acta 20:1149–1173.

Frost RL, Vassallo AM. 1996. The dehydroxylation of the kaolinite clay minerals using infrared emission spectroscopy. Clays Clay Miner 44:635–651.

Frost RL, Fredericks PM, Bartlett JR. 1993. Fourier transform Raman spectroscopy of kandite clays. Spectrochim Acta 20:667–674.

Frost RL. 1995. Fourier transform Raman spectroscopy of kaolinite, dickite and halloysite. Clays Clay Miner 43:191–195.

Frost RL. 1997. The Structure of the kaolin clay minerals—An FT Raman study. Clay Miner 32:73–85.

Frost RL, van der Gaast SJ. 1997. Kaolinite hydroxyls—A Raman microscopy study. Clay Miner 32:293–306.

Frost RL. 1998. Hydroxyl deformation in kaolinites. Clays Clay Miner 46:280–289.

Giese RF. 1988. Kaolin minerals: Structures and stabilities. Rev Mineral 19. In: Bailey SW, editor. Hydrous phyllosilicates. Mineral Soc Am. Chelsea, MI: BookCrafters. p 29–66.

Hess CA, Saunders VR. 1992. Periodic *ab initio* Hartree-Fock calculations of the low symmetry mineral kaolinite. J Phys Chem 96:4367–4374.

Hinckley DN. 1963. Variability in "crystallinity" values among the kaolin deposits of the coastal plain of Georgia and South Carolina. Clays Clay Miner 11:229–235.

Hunt GR, Hall RB. 1981. Identification of kaolins and associated minerals in altered volcanic rocks by infrared spectroscopy. Clays Clay Miner 29:76–78.

Hunt GR, Ashley RP. 1979. Spectra of altered rocks in the visible and near infrared. Econ Geol 74:1613–1629.

Hunt GR, Salisbury JW, Lenhoff CJ. 1973. Visible and near-IR spectra of minerals and rocks. VI. Additional silicates. Modern Geol 4:85–106.

Johansson U, Holmgren A, Forsling W, Frost RL. 1998. Isotopic exchange of kaolinite hydroxyl protons—A diffuse reflectance infrared Fourier transform spectroscopic study. Analyst 123:641–645.

Karakassides K, Petridis D, Gournis D. 1997. Infrared reflectance studies of thermally treated Li- and Cs- montmorillonites. Clays Clay Miner 45:649–658.

Lazarev AN. 1972. Vibrational spectra and structure of silicates. New York: Plenum Pr. p 178–182.

Lindberg JD, Snyder DG. 1972. Diffuse reflectance spectra of several clay minerals. Am Mineral 57:485–493.

Matsunaga T, Uwasawa M. 1993. Near infrared diffuse reflectance spectra of clay minerals. Nippon Dojo Hiryogaku Zasshi 64:329–331.

Michaelian KH, Bukka K, Permann DNS. 1987. Photoacoustic infrared spectra (250–10,000 cm^{-1}) of partially deuterated kaolinite #9. Can J Chem 65:1420–1423.

Michaelian KH. 1986. The Raman spectrum of kaolinite #9 at 21 °C. Can J Chem 64:285–289.

Tanabe K, Uesaka H, Inoue T, Takahashi H, Tanaka S. 1994. Identification of mineral components from near infrared spectra by a neural network. Bunseki Kagaku 43:765–769.

Yvon J, Lietard O, Cases JM, Delon JF. 1992. Minéralogie des argiles kaoliniques des Charentes. Bull Mineral 105: 417–581.

(Received 18 August 1997; accepted 5 January 1998; Ms. 97-076)